Environmental Science and Pollution Research (2020) 27:26239–26248
https://doi.org/10.1007/s11356-020-08940-9

RESEARCH ARTICLE

Photocatalytic degradation of methyl orange from wastewater using a newly developed Fe-Cu-Zn-ZSM-5 catalyst

Mushtaq Ahmad[1] · Abdul Raman Abdul Aziz[1] · Shaukat Ali Mazari[2] · Abdul Ghaffar Baloch[3] · Sabzoi Nizamuddin[4]

Received: 4 October 2019 / Accepted: 17 April 2020 / Published online: 2 May 2020

Abstract

Photo-Fenton oxidation is one of the most promising processes to remove recalcitrant contaminants from industrial wastewater. In this study, we developed a novel heterogeneous catalyst to enhance photo-Fenton oxidation. Multi-composition (Fe-Cu-Zn) on aluminosilicate zeolite (ZSM-5) was prepared using a chemical process. Subsequently, the synthesized catalyst was characterized by using X-ray diffraction (XRD), field emission scanning electron microscope (FESEM), high-resolution transmission electron microscopy (HRTEM), energy dispersive X-ray (spectroscopy) (EDX), and Brunauer–Emmett–Teller (BET). Activity of the synthesized catalyst is analysed to degrade an azo dye, methyl orange. Taguchi method is used to optimize color removal and total carbon content (TOC) removal. The dye completely degraded, and 76% of TOC removal was obtained at optimized process conditions. The amount of catalyst required for the desired degradation of dye significantly reduced up to 92% and 30% compared to conventional homogenous and heterogeneous Fenton oxidation processes, respectively.

Keywords Heterogeneous Fenton process · Taguchi method · HZSM-5

Introduction

With the rapid development of industry, water pollution is increasing due to addition of synthetic pollutants. Major part of these synthetic pollutants includes different kinds of dyes, which come from the textile, leather, and food industries. These types of pollutants are hazardous for human beings (Znad et al. 2018; Vaez and Javanbakht 2020).

Responsible editor: Suresh Pillai

✉ Shaukat Ali Mazari
shaukat.mazari@duet.edu.pk

✉ Sabzoi Nizamuddin
nizamuddin.nizamuddin@rmit.edu.au

[1] Department of Chemical Engineering, Faculty of Engineering, University of Malaya, 50603 Kuala Lumpur, Malaysia

[2] Department of Chemical Engineering, Dawood University of Engineering and Technology, Karachi 47800, Pakistan

[3] Department of Mechanical Engineering, Quaid-e-Awam University of Engineering, Science and Technology, Nawabshah, Sindh, Pakistan

[4] School of Engineering, RMIT University, Melbourne, VIC 3000, Australia

Azo dyes are generally classified as cationic- or anionic-based. Anionic-based azo dyes such as methyl orange (MO) are particularly difficult to be decomposed at ambient condition using conventional methods including adsorption, reverse osmosis, and coagulation (Liu et al. 2018). These processes can just accumulate MO-like pollutants instead of decomposing them. To overcome these issues, advance oxidation processes are used to treat industrial wastewater (Kiss et al. 2006; Liotta et al. 2009; Abdullah and Wong 2010; Bolova et al. 2011; Karthikeyan et al. 2012). Integration of UV is considered to maximize Fenton oxidation (Heng et al. 2013; Szeto et al. 2018). Similarly, the heterogeneous catalysts with controlled surface morphological properties, molecular homogeneity, and chemical composition are considered and modified to effectively degrade the MO-like pollutants.

Researchers have been able to tailor the characteristics of the materials since the advent of nanotechnology to achieve separation and purification goals (Deutschmann et al. 2009; Rodríguez-Chueca et al. 2015). However, it is still challenging to get control on desired properties of the materials and cost-effectiveness due to inherent physical and chemical properties of the bulk ingredients (Thomas and Thomas 2014; Heggo and Ookawara 2017).

Metal organic frameworks (MOFs) have been introduced to overcome these problems for preparation of heterogeneous

catalysts. MOFs have been reported to improve the efficacy, lifetime, and catalyst reusability (Yang et al. 2011; Wang et al. 2017. Such approaches are favorable for syntheses of some explicit catalysts, however, may not help in producing a wider variety of heterometallic catalysts. Recently, we have developed a novel two-step method to produce heterometallic catalysts with improved properties (Ahmad and Abdul Aziz 2015; Ahmad et al. 2015). The process is utilized to produce Fe-ZSM-5 catalyst. The produced catalyst was effectively utilized for degradation and decolorization of wastewater containing organic recalcitrant contaminants through Fenton oxidation process (Ahmad et al. 2015). The effect of dye/catalyst (wt/wt), initial concentration of dye, reaction time, catalyst/H_2O_2 (wt/wt), temperature, and pH was optimized. The promising results were obtained through 100% degradation of dye and 77% of mineralization efficiency was achieved against Acid Blue 113.

In this study, two-step process developed previously is employed to produce Fe-Cu-Zn-ZSM-5 catalyst which provides many advantages over the other heterogeneous catalysts (Nguyen et al. 2011; Jaafar et al. 2012; Khaki et al. 2015). Synthesized catalyst is characterized for morphology and structure, particle size distribution, thermogravimetric analysis, and surface area. The stability and activity of catalyst synthesized are also evaluated against methyl orange.

Methodology

Materials

In this study, all the purchased chemicals and materials were directly used, without further purification. Methyl orange containing two azo bonds (Fig. 1) was chosen as the recalcitrant dye and was acquired from Sigma-Aldrich. H_2O_2 30% (wt/wt) 2,2′-bipyridine, iron chloride, zinc chloride, copper chloride, and 2-propanol were purchased from Merck Sdn Bhd. Malaysia. ZSM-5 was obtained from Zeolyst International.

Preparation of catalyst

Fe-Cu-Zn-ZSM-5 was produced though the two-step process. This process was developed and optimized for production of nano-size supported- and unsupported-type heterometallic catalysts (Ahmad and Abdul Aziz 2015). At first, monometallic organic frameworks were synthesized through reacting 2,2′-bipyridine with metal chlorides in 2-propanol. Fe-MOF was synthesized using 8.5 g of 2,2′-bipyridine and 3.6 g of $FeCl_2.4H_2O$ was dissolved (individually) in 30 mL of 2-propanol and reacted though dropwise mixing in a lab-scale reactor. The reaction mixture was continuously stirred at 36 °C for 3 h. Precipitated crystals of $[Fe(byp)_2]Cl_2$ were separated by using vacuum filtration and washed with ethanol and ether to eliminate impurities. The yield of Fe-MOF was 78.5%.

Similarly, $[Zn(bpy)_2]Cl_2$ and $[Cu(bpy)]Cl_2$ were synthesized by using 3.13 g of $ZnCl_2$ and 7.0 g of 2,2′-bipyridine ligand, while 3.8 g of $CuCl_2.2H_2O$ and 7.0 g of 2,2′-bpy ligand were used to synthesize $[Cu(bpy)]Cl_2$ (Ahmad et al. 2015). Fine crystals of $[Zn(bpy)]Cl_2$ and $[Cu(bpy)]Cl_2$ were separated and washed with ether to remove impurities. The yields were 80% and 78%, respectively.

In the second step, the ZSM-5 zeolite matrixes were impregnated with mono-metallic-MOFs. The concentrations of the metallic complex were adjusted to obtain 2.5%, 2%, and 1% of Fe, Cu, and Zn (wt/wt) in the final composition of catalyst. After impregnation, the solid material was filtered, dried for 12–14 h (at 100 °C), and then placed in furnace for calcination for 7–8 h. The temperature was gradually increased and finally maintained at 650 °C. Air flow was also adjusted to completely remove the ligand part.

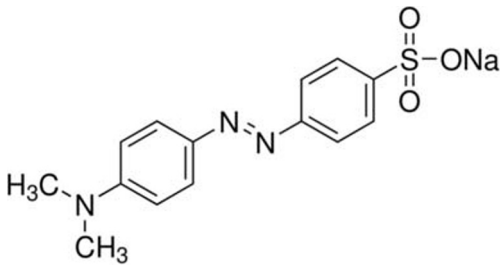

Fig. 1 Chemical structure of methyl orange

Characterization

ZSM-5-supported and the synthesized MOFs and catalysts were analyzed by using EDX, FESEM, FTIR, HRTEM, and BET instruments. Composition and surface morphology of the ZSM-5, MOFs, and Fe-ZSM-5 were studied by using Phenom ProX FESEM. JEOL JEM2100-F was used for HRTEM analyses. Perkin Elmer FTIR-spectrum 400 was used for FTIR analysis to observe the shifts due to coordinate bonding in MOFs and development of the new chemical structure of Fe-Cu-ZSM-5.

Surface Area and Porosity Analyzer (ASAP 2020) was used to analyze the surface area of ZSM-5 matrix and synthesized Fe-ZSM-5 catalyst. Surface area and pore width were determined by using the BET technique. Pore volumes were analyzed by using N_2 adsorption-desorption curves. Similarly, micropore volumes were calculated by the t-plot schemes.

Experimental design

Experiments for Fenton oxidation were designed using the Minitab 16 with Taguchi method. In the case of photocatalytic Fenton oxidation process, initial concentration of the dye, pH,

catalyst loading, quantity of oxidizing agent, process time, temperature, reactor size, geometry, UV light, and feed flow play an important role. However, in this study, the aim of the research was to evaluate the activity of the synthesized materials produced from newly developed process. To serve the purpose, a batch reactor was used, in which reactor size is already fixed. In addition, there were also no possibilities to change flow or flow locations; therefore, in addition to authors' previously published work (Ahmad et al. 2015; Ahmad et al. 2016), a set of preliminary experiments were also conducted to design the Fenton experiments. Catalyst loading, H_2O_2, reaction time, and pH were selected as the process variables. Similarly, the dye degradation and total carbon content (TOC) reduction were selected as the output responses. Three levels of each parameter were chosen (Table 1). Taguchi scheme suggested a total of 9 experiments.

A stirred tank reactor (500 mL capacity) placed inside a UV-integrated system was used for carrying out experiments. Two UV lamps with each 50 W and 15 W were used to analyze the photo catalytic activity of the catalyst. Solutions of 0.5 M sulfuric acid (H_2SO_4) and 1 M sodium hydroxide (NaOH) were used to maintain the initial pH of the dye solution. A digital pH meter (Cyberscan pH 300, Eutectic Instruments) was used to measure pH.

To determine the adsorption rate of the selected dye, earlier, a set of experiments was conducted. A solution of 100 mg/L of methyl orange was prepared and treated in the dark for 4 h. An optimized amount of each catalyst was added in each experiment based on the findings of our previous work (Ahmad et al. 2015). After the experiments, the samples were centrifuged, filtered, and scrutinized for decolorization.

In the second set of experiments, the synthesized catalysts were evaluated under photo-Fenton oxidation conditions. The used amount of catalyst and H_2O_2 is given in Table 2. The 0.20-μm Millipore syringe filters were used for the filtration of samples and analyzed through Merck UV spectrophotometer (Spectroquant Pharo 300). Equation (1) has been used for the degradation of the treated samples:

$$Degradation\ (\%) = \left(1-\frac{C_t}{C_o}\right) \times 100 \quad (1)$$

Table 1 Design factors and their levels

Operating parameters	Level 1	Level 2	Level 3
Catalyst (wt. in mg)	67	100	133
H_2O_2 (mL)	2	5	10
pH	3	5	9
Time (h)	1	2.5	4

where C_o and C_t are the starting and final concentrations, estimated through the UV spectrophotometer, observed at λ_{max} for the selected dye.

TOC analyzer (Shimadzu-00077) was used for the analyses of total organic content (TOC) removal considering the difference between the total carbon (TC) content and inorganic carbon (IC) content. Equation (2) illustrates the percentage reduction in TOC values.

$$TOC(\%) = \left(1-\frac{TOC_f}{TOC_o}\right) \times 100 \quad (2)$$

Furthermore, to identify the concentration of by-products and intermediates of Fenton oxidation, high-performance liquid chromatography (HPLC, Agilent technology 1200 series) with separation column C18 (4.6 mm × 150 mm × 5 μm) was used. Acetonitrile/water (v/v) was used at a ratio of 60/40 as the mobile phase. The flow rate of mobile phase was maintained at 1 mL/min. To analyze the unknown compounds after degradation, the HPLC was calibrated using standard analytical reagents like benzene, phenol, aniline, hydroquinone, catechol, benzoquinone, formic acid, oxalic acid, and malic acids. The compounds produced during Fenton oxidation were identified by matching the retention times of standard reagents, calibrated under similar conditions (Ajeel et al. 2015).

Results and discussion

Catalyst characterization

Surface area, elemental composition, pore volume, and particles size were analyzed for synthesized catalysts. SEM images for Fe-Cu-Zn-ZSM-5 are exhibited in Fig. 2. Formation of nano-sized metal oxide particles on the ZSM-5 matrix and inside the matrix has been witnessed due to thermal decomposition of impregnated MOFs.

Surface microstructures of all the synthesized MOFs, catalyst, and the morphology of the parent ZSM-5 are presented through FESEM and HRTEM analyses (Fig. 2). The morphology of the parent ZSM-5 (Fig. 2(d)) greatly altered after the addition of metallic oxides via impregnation of MOFs and their thermal degradation (Fig. 2(e)). The calcination triggered thermal decomposition of MOFs, forming nano-sized heterometallic oxides on the zeolitic matrix as shown by the HRTEM results (Fig. 2(f)) (Chen, Chen et al. 2009).

Table 3 shows the composition of support, ZSM-5, and fabricated catalyst with the help of surface area method. The existence of iron, aluminum, silicon, zin, copper, and oxygen atoms in solid cluster indicates their elemental composition. In comparison with aluminum and integrated atoms, oxygen and silicon ratios were prominent. The elimination of the ligand

Table 2 Dye degradation and TOC removal from nine different experiments

R. no.	Catalyst (mg)	H_2O_2 (mL)	pH	Time (h)	Dye degradation (mg/mL)	TOC removal
1	67	2	3	1	74.00	58.00
2	67	5	5	2.5	35.13	20.35
3	67	10	9	4	94.13	65.73
4	100	2	5	4	32.04	18.00
5	100	5	9	1	51.50	16.98
6	100	10	3	2.5	98.61	50.00
7	133	2	9	2.5	28.95	22.13
8	133	5	3	4	99.07	74.17
9	133	10	5	1	70.74	27.94

part from the supporting matrix, producing nano-oxides on the surface of the support, is caused by calcination. The EDX values of the loaded Fe, Cu, and Zn (wt/wt) moieties (2.5%, 2.1%, and 0.9%) were in agreement with the theoretical values (2.5%, 2%, and 1%).

The specific surface area of the synthesized Fe-Cu-Zn-ZSM-5 catalyst (in m^2/g) was determined using the BET (Brunauer–Emmett–Teller) method. Presence of metallic oxide nanoparticles lessen the surface area of Fe-ZSM-5 from 297.79 to 291.23 m^2/g. This study confirmed the filling of metal oxide nanoparticles in the pores of ZSM-5 support (Yan et al. 2014).

The comparison of synthesized catalysts together with ZSM-5 through XRD patterns is presented in Fig. 3. Distinctive diffractograms of the ZSM-5 are 2 = 7–9° and 23–25° of synthesized catalysts (Cihanoglu et al. 2015). The results indicated that the loading of Fe, Zn, Ni, and Cu MOFs and their nano-oxides did not damage the crystallinity of the matrix at accessible positions inside the zeolite, whereas filling of metallic nano-oxides into the zeolite matrix of ZSM-5 altered the intensities of characteristic peaks. Fe and Zn nano-oxide particles reduced the characteristic peak intensities as indicated by X-ray absorption (Ni et al. 2011; Cihanoglu et al. 2015). Similar trends have also been reported in literature (Heemsoth et al. 2001; Wang et al. 2017; Li et al. 2009). Ni et al. (2011) reported that distribution of Fe and Zn nano-oxide particles cannot alter the crystallinity of the matrix instead change the catalyst; in particular, ZnO impregnation reduces the quantity of Brønsted acid sites while increasing Lewis acid sites (Wang et al. 2007; Ni et al. 2011).

The mixing and washing away of non-uniform aluminum grown zones from the ZSM-5 matrix have been attributed for the reduction in particle size, which lead to the reduction in peak intensities. Furthermore, amorphous oxide phases on the zeolite surface may have decreased the peak intensities (Dukkancı et al. 2010; Cihanoglu et al. 2015), whereas addition of Cu along with Fe, and Zn, nano-oxide particles somewhat improved the peak intensities (Villa et al. 2005; Dukkancı et al. 2010).

Photodegradation experiments

To degrade and decolorize methyl orange, photo-Fenton oxidation was carried out. Table 2 illustrates the comparison of these experiments. In experiments 3, 6, and 8, color was completely removed, whereas TOC removal was 66%, 50%, and 74% for methyl orange. When the nano-particles of metal oxides are irradiated by light having energy equal or greater to their band gap, valance electrons become excited to conduction band, with simultaneous generation of holes in the valance bond. These photo-generated electron-hole pairs can either interact with other molecules or recombine. The holes in the valance bond can react with water or hydroxide ions to form reactive $^*OH$ radicals while electrons are used to produce superoxide radical anions (Yu et al. 2012; Khaki et al., 2015). These radicals may generate peroxides and H_2O_2 in the presence of organic scavenger. The hydroxyl radicals attack the dye molecules to give oxidized product (Kaur et al. 2013). Equations 3–10 illustrate the reaction mechanism.

$$M_XO_Y + h\nu \rightarrow h^+ + e^- \quad (3)$$

$$h^+ + e^- \rightarrow \text{heat} \quad (4)$$

$$H_2O + h^+ \rightarrow H^+ + OH^* \quad (5)$$

$$h^+ + OH^- \rightarrow OH^* \quad (6)$$

$$e^- + O_2{}^- \rightarrow O_2{}^{-*} \quad (7)$$

$$O_2{}^{-*} + H_2O \rightarrow H^+ + H_2O_2 + \quad O_2 \quad (8)$$

$$O_2{}^{-*} + \text{Organic compound} \rightarrow \text{Organic compound} : OO^- \quad (9)$$

$$OH^- + \text{Organic compound} \rightarrow \text{oxidized product} \quad (10)$$

where M is the notation for Fe, Cu, and Zn; and X and Y represent the number of atoms in oxide. It was revealed that degradation of methyl orange–type azo dye is also favored by alkaline medium (Kaur et al. 2013). HPLC study detected traces of carboxylic acid, aniline, and benzoquinone. The oxidative splitting of the dye amino benzene moiety forms a $^oNH\text{-}C_6H_5$ radical which has potential

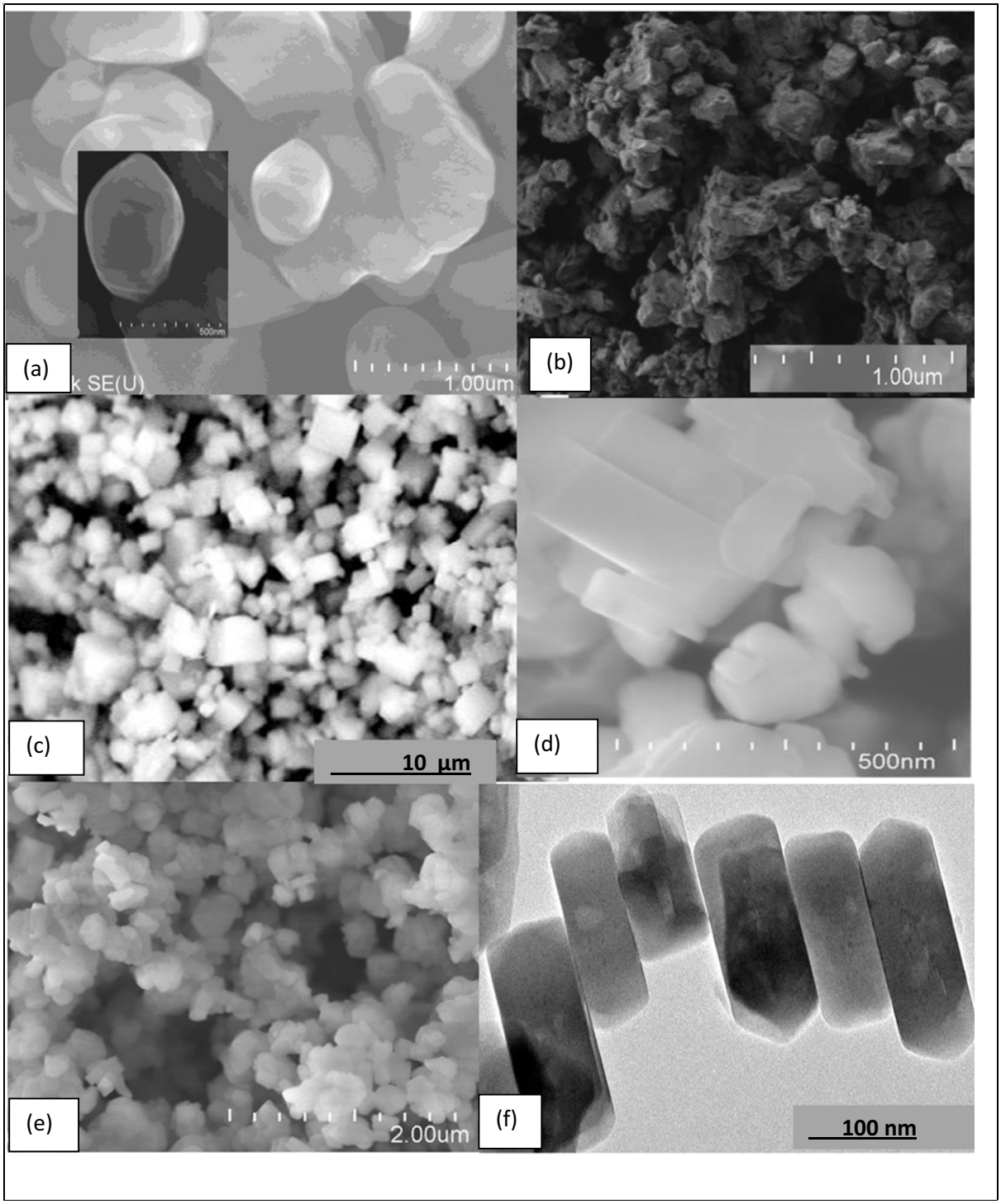

Fig. 2 FESEM images of Cu complex (a), Zn complex (b), Fe complex (c), ZSM-5 (d), and synthesized Fe- Cu-Zn-ZSM-5 (e) and HRTEM images of the synthesized Fe-Cu-Zn-ZSM-5 catalyst (f)

to abstract an amino hydrogen atom from dye molecules leading to the formation of aniline (Zayani et al., 2008; Ahmad et al. 2015). The additional perceived moiety was benzoquinone, which is achieved by degradation of benzene and phenol (Zayani et al. 2008; Gomathi Devi et al. 2009; Ajeel et al. 2015). Further, it can be recommended that oxidation reaction results in splitting of benzoquinone ring to formic acid and maleic acid (Ajeel et al. 2015). The findings of this study are observed in the literature (Ahmad et al. 2015).

Table 3 EDX analysis of Fe-Cu-Zn-ZSM-5

Catalyst cluster	Weight composition (%)					
	Si	Al	O	Fe	Cu	Zn
Fe-Zn-Cu-ZSM-5	43.0	1.9	49.60	2.6	2.1	0.9
ZSM-5	19.6	3.4	71.8	–	–	–

Effect of process parameters

Initially, 100 mg/L of dye concentration was examined for removal of methyl orange, which removed up to 72% in 4 h. It is supposed that complete removal capacity is achieved as equilibrium was achieved, and no further changes were observed after 4 h. The synthesized Fe-Cu-Zn-ZSM-5 illustrated a noticeable removal performance for methyl orange. Several researchers have described that different dyes have different removal efficiency even with the same catalyst due to dissimilar organic structures. Furthermore, various binding affinities with the surface of Fe-ZSM-5 may have also been affected due to different functional groups like NH_2, SO_3^-, and OH (Zhou et al. 2013, Shirzad-Siboni et al. 2014).

Effect of catalyst loading

To understand the effect of synthesized Fe-Cu-Zn catalyst on photodegradation of MO, the catalyst range was set between 67 and 133 mg/100 mL of dye solution (Table 1). With smaller amount of catalyst, the rate of color removal was faster; however, the TOC removal was relatively slow. By increasing the catalyst from 67 to 100 mg/100 mL of solution, the degradation rate was constant but increasing the catalyst amount to 133 mg/100 mL of solution, the rate increased, and the curve showed a steep trend (Fig. 4). This increase in dye degradation may be attributed to increased active sites, formed through the integration of nano-oxides in zeolitic matrix (Kaur et al. 2013). Such trend of oxide filling in zeolitic matrix was reported in literature (Heemsoth et al. 2001; Wang et al. 2007; Li et al. 2009). Ni et al. (2011) revealed that distribution of nano-oxide particles of Zn and Fe resulted in significant alteration of acid sites. Specifically, impregnation of ZnO resulted in reduction of sites of Brønsted acid. Though, sites of Lewis acid were significantly increased (Wang et al. 2007; Ni et al. 2011).

This causes formation of increased hydroxyl radicals which are responsible for the degradation of dyes (Gomathi Devi et al. 2009). However, by increasing the catalyst amount, turbidity of the dye solution also increased. It had resulted less UV penetration and favored the light scattering, which leads to reduction in dye degradation (Kaur et al. 2013).

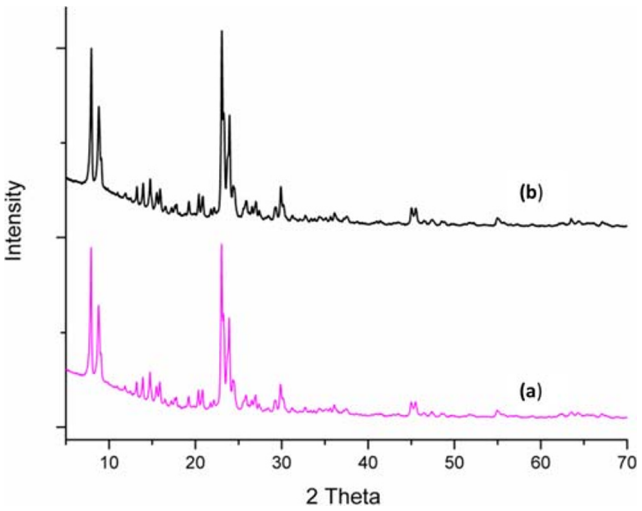

Fig. 3 XRD pattern of ZSM-5 (a) and synthesized Fe-Zn-Cu-ZSM-5 (b)

Effect of oxidizing agent

The range of H_2O_2 (33 mg/L of stock solution concentration) was set between 2 and 10 mL/100 mL of dye solution. Increasing the H_2O_2 from 2 to 10 mL/100 mL of solution, degradation rate increased. This may be due to the increased formation of hydroxyl radicals, which are responsible for dye degradation (Gomathi Devi et al. 2009; Jaafar et al. 2012, Yu et al. 2012). However, excess amounts of H_2O_2 alter the H_2O_2/catalyst ratios resulting in reduced decolorization of MO. With excess amount of H_2O_2, hydroxyl radicals' production quenches down which ultimately leads to reported effect. It is also observed that decomposition of H_2O_2 leads to the formation of O_2, particularly at higher pH values. This facilitates the conversion of ferrous ions into ferric-hydroxo complexes, which slowdown the decolorization and degradation of MO dye. Literature also shows that, at higher temperatures, increasing H_2O_2 has no significant effects or even have adverse effect. This might be attributed to higher temperature favoring the thermal decomposition of H_2O_2, which reduces the availability of H_2O_2 for the formation of hydroxyl radicals (Ahmad et al.). Results exhibit that H_2O_2 had significantly contributed to the degradation of MO, even more than the amount of catalyst and process time.

Effect of pH

To study pH effect on photodegradation of MO, the range of pH was set between 3 and 9 (Table 1). Maximum efficiency of mineralization was obtained at a pH value of 3. However, by increasing the pH value to 5, the degradation rate decreased. It is also observed that increase in pH facilitates the conversion of ferrous ions into ferric-hydroxo complexes, which slowdowns the decolorization and degradation of MO dye. However, by further increasing pH up to 9, the degradation rate again increases. It may be

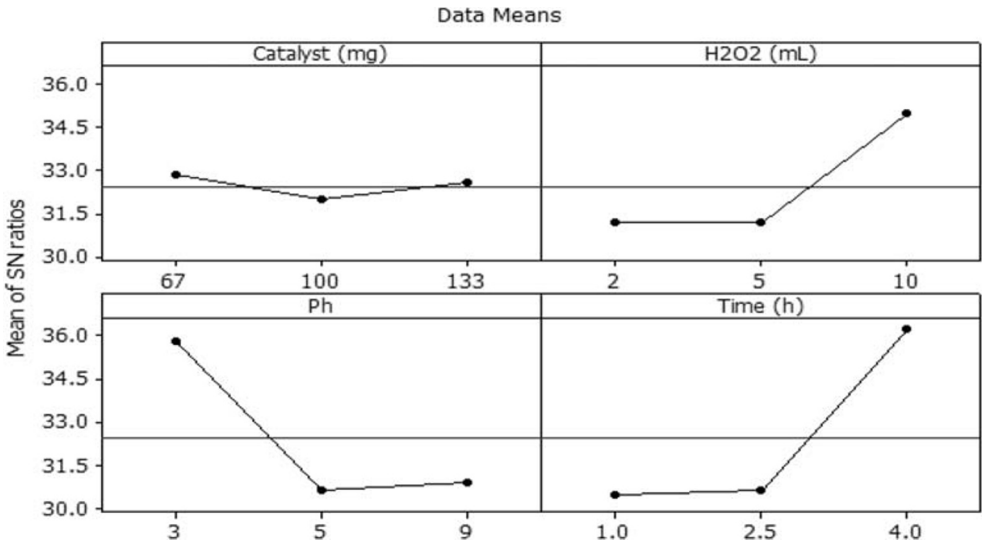

Fig. 4 Mean TPCI plots against different factors levels

attributed that alkaline medium also facilitates the formation of $^{-}$OH ions, which further caused to form the *OH radicals. These radicals enhance photodegradation (Gomathi Devi et al. 2009; Kaur et al. 2013). Znad et al. (2018) examined the photodegradation of the MO with TiO2/-ZSM catalyst and reported that the decolorization increases with the increase in pH from 2.0 to 7.5 and decreases onward. The authors claimed that, under acidic conditions (pH < 6), adsorption of H^{+} ions dominates, which makes the positive charge on catalyst surface, whereas adsorption of $^{-}$OH ions makes negatively charged surface under alkaline conditions. Based on these charges, authors suggested two different mechanisms for the photodegradation of dye. First one deals with direct oxidation by positive holes while other indicates MO degradation with direct reduction by electrons (Znad et al. 2018).

For the current study, pH effect on dye degradation was found to be substantial, whereas the loading of catalyst had lesser influence than the other three factors.

Effect of time

Reaction time is one of the important parameters in Fenton oxidation process. In this study, time ranged from 1 to 4 h (Table 1). In runs 3 and 8 (Table 2), the effect of time is significant. With increase in the time, degradation of the dye increased (Fig. 3). It is noted that, after 30 min, the color was completely removed. During oxidation process, time for HO radical formation is important for which interaction of catalyst surface and H_2O_2 is required. Although, after radical formation, less time is required for decolorization. However, for removal of TOC, more time is required. TOC removal efficiency indicates the reduction in total organic compounds present in wastewater. HPLC analysis showed traces of several compounds (carboxylic acid, benzoquinone, and aniline) as by-products and intermediates of photodegradation of MO. This indicates that complete TOC removal is not possible even after 4-h treatment. Literature also supports these findings (Znad et al. 2018; Vaez and Javanbakht 2020). Several studies

Table 4 The obtained S/N ratios and their normalized and TPCI values

Run	S/N ratio	Normalized S/N ratio			TPCI
	Dye degradation	TOC removal	Dye degradation	TOC removal	
1	37.38	35.27	0.47	0.92	0.89
2	30.91	26.17	− 1.02	− 0.84	− 1.23
3	39.47	36.36	0.95	1.13	1.35
4	30.11	25.11	− 1.21	− 1.05	− 1.49
5	34.24	24.60	− 0.26	− 1.14	− 0.87
6	39.88	33.98	1.04	0.67	1.14
7	29.23	26.90	− 1.41	− 0.70	− 1.42
8	39.92	37.40	1.05	1.33	1.55
9	36.99	28.92	0.38	− 0.31	0.08

show that, with complete consumption of Fe^{+2}, even with longer time, degradation and mineralization decrease.

Optimization study

In this work, the Taguchi method was used to optimize TOC reduction and methyl orange degradation. The details of the experiments and findings are presented in Table 4. The responses received as a result of photo-Fenton oxidation process were changed to S/N ratios. High values of TOC reduction and methyl orange degradation were desired; therefore, option "larger the better" S/N ratio was chosen. For runs 3 and 8, these values remained highest. Synthesized Fe-Cu-Zn-ZSM-5 enabled to completely degrade the selected dye (100 mg/L) along with 74% of TOC reduction at pH 3. However, getting optimized conditions for every experiment's response was not feasible; therefore, obtained S/N ratios were optimized initially and then transformed to a component known as "Total Principal Component Index (TPCI)" with the help of principal component analysis (French and Czernik 2010; Ahmad et al.).

The S/N ratio was normalized at each level, followed by application of principal component analysis to normalized data through matrix $\overline{X}$. Then, matrix $\overline{X}$ was transformed to covariance matrix (Cx), which was used for calculating the Eigen values for suggested responses. The system changes normalized S/N ratio to set of non-correlated components. The "Eigen value" as greater than 1 was chosen for such calculations. The theoretical details about every step are reported in the literature (Ahmad et al.). Finally, the following overall influencing trend was noticed for the process parameters:

pH > H_2O_2 > time > catalyst amount.

The pH effect on dye degradation was found to be substantial, whereas the loading of catalyst had less influence than the other three factors. On the other hand, all parameters had vital effect on the degradation of dye. The findings obtained in this study are similar to previous study reported in the literature (Ahmad et al.). In addition, integration of UV with heterogeneous Fenton (with the synthesized catalyst) resulted in an increase of 10% in the process efficiency as compared with heterogeneous Fenton processes without UV.

Efficiencies of the synthesized catalysts were then measured at the optimized values (summarized and provided in Table 5). Figure 5 shows the dye degradation and TOC removal at optimized conditions. It was observed that dye was

Table 5 Optimized conditions for photo-Fenton oxidation

Dye mg/L	Catalyst wt	H_2O_2 mL	pH	Time H
100	133	10	3	4

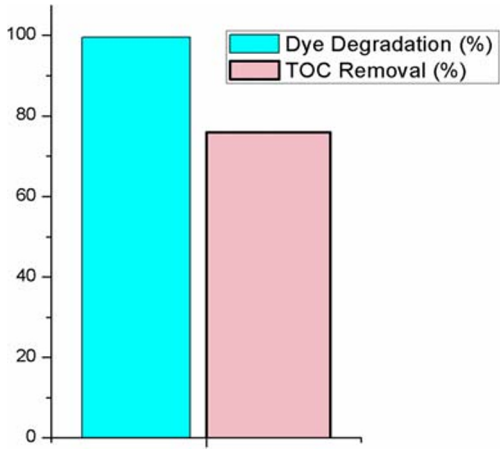

Fig. 5 Dye degradation (%) and TOC removal at optimized process values

fully degraded on these conditions, yielding 99.5% degradation efficiency and 76% TOC removal. UV-integrated system improved the Fenton oxidation with a significant increment of 10%. Overall, it was analyzed that combining UV light and Fe-Cu-Zn-ZSM-5 catalyst has enhanced the process efficiency.

In addition to catalytic activity, stability and reusability of the synthesized catalysts are also important. The leaching of impregnated metal ions from zeolites matrix during treatment process decreases the catalyst stability. A catalyst with minimal leaching is considered as a firm catalyst (Yan et al. 2014). Generally, leaching is measured directly using ICP (Ahmad et al. 2016) or indirectly (Ahmad et al.) by using FTIR-, EDX-, and SEM-based techniques. In this study, ICP analysis revealed that at pH 9 and 5 the leaching of metal from ZSM-5 matrix was below 2 ppm. However, at pH 3, leaching rate was observed relatively high (4.2 ppm). These values slightly increased from the permissible limit (< 2 ppm); however, the present leaching results are better than several other studies (Chen et al. 2008; Grcic et al. 2009; Dukkancı et al. 2010; Yan et al. 2016).

To examine the efficiency and reusability, the recovered catalysts from the treated solutions were dried at 200 °C for 2.5 h and were used under similar process conditions. Even after three trials, catalytic behavior of the synthesized catalyst was observed stable and reproduceable. Reduction in the efficiency of the reused catalyst was not more than 5%, which shows that deactivation either due to in situ transformation or metal leaching is insignificant. Literature shows that, although utilization of UV enhances the degradation rate, the treatment cost also increases significantly (Zhou et al. 2013). A comparison on the decolorization and TOC/COD removal efficiency using different heterometallic catalysts is given in Table 6. Comparison includes different process parameters and reactor geometries. To overcome these limitations, 1 L of the MO dye solution was taken as basis and examining the influencing

Table 6 Comparisons of synthesized catalyst with other heterometallic catalysts

Dye	Dye conc. (mg/L)	FeZSM-5 wt (mg/L)	H_2O_2 wt (mg/L)	pH	Time h	Decolorization %	TOC/COD removal %	Reference
MO	100	1330	5440	3	4	99.0	77 (TOC)	Present study
MO	20	2000		2	3	99	42 (TOC)	(Znad et al. 2018)
Mo	10	1400			4	82		(Qiu et al. 2019)
MO	5	70		11	2	90		(Vaez and Javanbakht 2020)
MO	50	1000	17.6	2	0.5	100	74.5 (COD)	(Liu et al. 2018)
MO	200	1000	1020	5.8	2	99.0	64 (TOC)	(Zhou et al. 2013)

factors such as catalyst amount, initial dye concentration, H_2O_2, and pH, catalysts' efficiencies were compared.

Conclusions

In this work, a two-step chemical process was extended to synthesize the Fe-Cu-Zn-ZSM-5 catalyst. Subsequently, the catalyst was characterized using XRD, HRTEM, FESEM, EDX, and BET methods. The catalytic activity of the synthesized heterometallic material was evaluated under photo-Fenton conditions, against the recalcitrant wastewater containing methyl orange as model azo dye.

The synthesized catalyst has shown noticeable performance, yielding 99% of dye degradation and 76% of TOC reduction under optimized process conditions . However, complete removal of TOC was not observed. In addition, integration of UV with heterogeneous Fenton resulted an increase of 10% in the process efficiency as compared to heterogeneous Fenton processes without UV. The stability and reusability of synthesized Fe-Cu-Zn-ZSM-5 in photo-Fenton oxidation were found economical and may reduce the consumption of the heterogeneous catalysts.

Funding information This research is financially supported by University of Malaya High Impact Research Grant (HIR-D000038-16001) provided by the Malaysian Ministry of Education.

References

Abdullah AH, Wong W-Y (2010) Decolorization of reactive orange 16 dye by copper oxide system. Sains Malays 39(4):587–591

Ahmad M, Abdul Aziz AR (2015) Elemental distribution and porosity enhancement in advanced nano bimetallic catalyst. Powder Technol 280(0):42–52

Ahmad M, Asghar A, Abdul Raman AA, Wan Daud WM (2015) Enhancement of treatment efficiency of recalcitrant wastewater containing textile dyes using a newly developed iron zeolite Socony Mobil-5 heterogeneous catalyst. PLoS One 10(10):e0141348

Ahmad M, Raman AAA, Basirun WJ, Bhargava SK (2016) Treatment of textile effluent containing recalcitrant dyes using MOF derived Fe-ZSM-5 heterogeneous catalyst. RSC Adv 6(56):51078–51088

Ajeel MA, Aroua MK, Daud WMAW (2015) Preparation and characterization of carbon black diamond composite electrodes for anodic degradation of phenol. Electrochim Acta 153:379–384

Bolova E, Gunduz G, Dukkanci M, Yilmaz S, Yaman YC (2011) Fe containing ZSM-5 zeolite as catalyst for wet peroxide oxidation of Orange II. Int J Chem React Eng 9(1):1-20

Chen A, Ma X, Sun H (2008) Decolorization of KN-R catalyzed by Fe-containing Y and ZSM-5 zeolites. J Hazard Mater 156(1):568–575

Chen H, Chen J, Wang R (2009) A structural study of the Fe/ZSM-5 catalyst by through-focus exit-wavefunction reconstruction in HRTEM. Microporous Mesoporous Mater 120(3):472–476

Cihanoglu A, Gunduz G, Dukkancı M (2015) Degradation of acetic acid by heterogeneous Fenton-like oxidation over iron-containing ZSM-5 zeolites. Appl Catal B Environ 165(0):687–699

Deutschmann O, Knözinger H, Kochloefl K., Turek T (2009). Heterogeneous catalysis and solid catalysts

Dukkancı M, Gunduz G, Yılmaz S, Yaman YC, Prikhod'ko RV, Stolyarova IV (2010) Characterization and catalytic activity of CuFeZSM-5 catalysts for oxidative degradation of Rhodamine 6G in aqueous solutions. Appl Catal B Environ 95(3–4):270–278

French R, Czernik S (2010) Catalytic pyrolysis of biomass for biofuels production. Fuel Process Technol 91(1):25–32

Gomathi Devi L, Girish Kumar S, Mohan Reddy K, Munikrishnappa C (2009) Photo degradation of methyl orange an azo dye by advanced Fenton process using zero valent metallic iron: influence of various reaction parameters and its degradation mechanism. J Hazard Mater 164(2–3):459–467

Grcic I, Muzic M, Vujevic D, Koprivanac N (2009) Evaluation of atrazine degradation in UV/FeZSM-5/H2O2 system using factorial experimental design. Chem Eng J 150(2–3):476–484

Heemsoth J, Tegeler E, Roessner F, Hagen A (2001) Generation of active sites for ethane aromatization in ZSM-5 zeolites by a solid-state reaction of zinc metal with Brønsted acid sites of the zeolite. Microporous Mesoporous Mater 46(2–3):185–190

Heggo D, Ookawara S (2017) Multiphase photocatalytic microreactors. Chem Eng Sci 169:67–77

Heng G, Malay C, Elmolla ES (2013). Combined UV/Fenton and SBR treatment of a semi-aerobic landfill leachate.

Jaafar NF, Jalil AA, Triwahyono S, Muhid MNM, Sapawe N, Satar MAH, Asaari H (2012) Photodecolorization of methyl orange over α-Fe 2 O 3-supported HY catalysts: the effects of catalyst preparation and dealumination. Chem Eng J 191:112–122

Karthikeyan S, Priya ME, Boopathy R, Velan M, Mandal A, Sekaran G (2012) Heterocatalytic Fenton oxidation process for the treatment of tannery effluent: kinetic and thermodynamic studies. Environ Sci Pollut Res 19(5):1828–1840

Kaur J, Bansal S, Singhal S (2013) Photocatalytic degradation of methyl orange using ZnO nanopowders synthesized via thermal decomposition of oxalate precursor method. Phys B Condens Matter 416(0):33–38

Khaki MRD, Sajjadi B, Raman AAA, Daud WMAW, Shmshirband S (2015) Sensitivity analysis of the photoactivity of Cu-TiO 2/ZnO during advanced oxidation reaction by adaptive neuro-fuzzy selection technique. Measurement 77 155-174

Kiss E, Vulic T, Reitzmann A, Lazar K (2006) Photo-Fenton catalysis for wet peroxide oxidation of phenol on Fe-ZSM-5 catalyst. Rev Roum Chim 51(9):931

Li Y, Liu S, Xie S, Xu L (2009) Promoted metal utilization capacity of alkali-treated zeolite: preparation of Zn/ZSM-5 and its application in 1-hexene aromatization. Appl Catal A Gen 360(1):8–16

Liotta L, Gruttadauria M, Di Carlo G, Perrini G, Librando V (2009) Heterogeneous catalytic degradation of phenolic substrates: catalysts activity. J Hazard Mater 162(2):588–606

Liu J, Peng G, Jing X, Yi Z (2018) Treatment of methyl orange by the catalytic wet peroxide oxidation process in batch and continuous fixed bed reactors using Fe-impregnated 13X as catalyst. Water Sci Technol 78(4):936–946

Nguyen TD, Phan NH, Do MH, Ngo KT (2011) Magnetic Fe2MO4 (M: Fe, Mn) activated carbons: fabrication, characterization and heterogeneous Fenton oxidation of methyl orange. J Hazard Mater 185(2–3):653–661

Ni Y, Sun A, Wu X, Hai G, Hu J, Li T, Li G (2011) The preparation of nano-sized H[Zn, Al]ZSM-5 zeolite and its application in the aromatization of methanol. Microporous Mesoporous Mater 143(2–3):435–442

Qiu L, Zhou Z, Yu Y, Zhang H, Qian Y, Yang Y, Duo S (2019) Fabrication of nanometer-sized high-silica SAPO-5 and its enhanced photocatalytic performance for methyl orange degradation. Res Chem Intermed 45(3):1457–1473

Rodríguez-Chueca J, Ormad MP, Mosteo R, Ovelleiro JL (2015) Kinetic modeling of Escherichia coli and Enterococcus sp. inactivation in wastewater treatment by photo-Fenton and H2O2/UV–vis processes. Chem Eng Sci 138:730–740

Shirzad-Siboni M, Jafari SJ, Giahi O, Kim I, Lee S-M, Yang J-K (2014) Removal of acid blue 113 and reactive black 5 dye from aqueous solutions by activated red mud. J Ind Eng Chem 20(4):1432–1437

Szeto W, Li J, Huang H, Leung DYC (2018) VUV/TiO2 photocatalytic oxidation process of methyl orange and simultaneous utilization of the lamp-generated ozone. Chem Eng Sci 177:380–390

Thomas JM, Thomas WJ (2014) Principles and practice of heterogeneous catalysis. John Wiley & Sons 768 pp

Vaez Z, Javanbakht V (2020) Synthesis, characterization and photocatalytic activity of ZSM-5/ZnO nanocomposite modified by Ag nanoparticles for methyl orange degradation. J Photochem Photobiol A Chem 388:112064

Villa AL, Caro CA, Correa CM d (2005) Cu- and Fe-ZSM-5 as catalysts for phenol hydroxylation. J Mol Catal A Chem 228(1–2):233–240

Wang L, Sang S, Meng S, Zhang Y, Qi Y, Liu Z (2007) Direct synthesis of Zn-ZSM-5 with novel morphology. Mater Lett 61(8–9):1675–1678

Wang W, Xu X, Zhou W, Shao Z (2017) Recent progress in metal-organic frameworks for applications in electrocatalytic and photocatalytic water splitting. Adv Sci 4(4):1600371

Yan Y, Jiang S, Zhang H (2014) Efficient catalytic wet peroxide oxidation of phenol over Fe-ZSM-5 catalyst in a fixed bed reactor. Sep Purif Technol 133:365–374

Yan Y, Jiang S, Zhang H (2016) Catalytic wet oxidation of phenol with Fe-ZSM-5 catalysts. RSC Adv 6(5):3850–3859

Yang SJ, Im JH, Kim T, Lee K, Park CR (2011) MOF-derived ZnO and ZnO@ C composites with high photocatalytic activity and adsorption capacity. J Hazard Mater 186(1):376–382

Yu L, Xi J, Li M-D, Chan HT, Su T, Phillips DL, Chan WK (2012) The degradation mechanism of methyl orange under photo-catalysis of TiO2. Phys Chem Chem Phys 14(10):3589–3595

Zayani G, Bousselmi L, Pichat P, Mhenni F, Ghrabi A (2008) Photocatalytic degradation of the Acid Blue 113 textile azo dye in aqueous suspensions of four commercialized TiO2 samples. J Environ Sci Health A 43(2):202–209

Zhou X, Cui X, Chen H, Zhu Y, Song Y, Shi J (2013) A facile synthesis of iron functionalized hierarchically porous ZSM-5 and its visible-light photocatalytic degradation of organic pollutants. Dalton Trans 42(4):890–893

Znad H, Abbas K, Hena S, Awual MR (2018) Synthesis a novel multilamellar mesoporous TiO2/ZSM-5 for photo-catalytic degradation of methyl orange dye in aqueous media. J Environ Chem Eng 6(1):218–227